

Regioselective hydrophenylation of olefins catalyzed by an Ir(III) complex

Takaya Matsumoto^{a,*}, Roy A. Periana^{b,c,1}, Douglas J. Taube^c, Hajime Yoshida^a

^a Central Technical Research Laboratory, Nippon Mitsubishi Oil Corporation, 8 Chidoricho, Naka-ku, Yokohama, Kanagawa 231-0815, Japan

^b Chemistry Department, Loker Hydrocarbon Institute, University of Southern California, Los Angeles, CA 90089, USA

^c Catalytica Advanced Technologies Inc., 430 Ferguson Drive, Mountain View, CA 94043, USA

Received 19 July 2001; received in revised form 17 August 2001; accepted 26 September 2001

Abstract

The novel, anti-Markovnikov, arylation of olefins with benzene to produce straight-chain alkylbenzenes with higher selectivity than branched alkylbenzenes is catalyzed by $[\text{Ir}(\mu\text{-acac-O,O',C}^3)(\text{acac-O,O'})_2(\text{acac-C}^3)]_2$ (acac = acetylacetonato), **1** [J. Am. Chem. Soc. 122 (2000) 7414]. The reaction of benzene with propylene gave *n*-propylbenzene and cumene in 61 and 39% selectivities, respectively. The reaction of benzene and styrene afforded 1,2-diphenylethane in 98% selectivity. Considering the anti-Markovnikov regioselectivity and lack of inhibition by water, we propose that the reaction does not proceed via a Friedel–Crafts, carbocation, mechanism. Complex **1**, amongst the various transition metal complexes examined, is the most efficient for catalyzing the anti-Markovnikov olefin arylation. The crystal structure of complex **1** was solved and is consistent with a binuclear Ir(III) structure with three different types of coordinated acac ligands as reported by earlier solution IR and NMR analyses. $[\text{Ir}(\mu\text{-acac-O,O',C}^3)(\text{acac-O,O'})\text{Cl}]_2$, **2**, was prepared by the reaction of complex **1** with benzoyl chloride, and the crystal structure was also reported. © 2002 Elsevier Science B.V. All rights reserved.

Keywords: Iridium complex; CH activation; Regioselective hydro phenylation; Anti-Markovnikov; Alkylation

1. Introduction

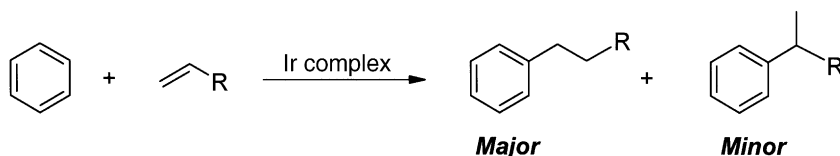
The alkylation of arene with olefins, catalyzed by Lewis and Brønsted acids (the Friedel–Crafts reaction) is a standard C–C bond forming reaction in the chemist's synthetic arsenal. Given the wide utility of this reaction, it is highly desirable to control both the regio and stereo selectivity of the reaction. With Friedel–Crafts catalysts the reaction proceeds via activation of the olefin and intermediate formation of carbocationic species. Consequently, the regioselectivity

for olefin addition is set by the relative stability of the carbocation intermediates which leads to regioselective formation of the more highly branched (Markovnikov), alkyl arene product. Additionally, stereoselective olefin addition is generally not possible in Friedel–Crafts alkylations, except for a recent report [2], due to the planarity of the geometry around the double bond of the olefin which generates intermediate carbocation. Given these considerations, it is clear that the development of new, alkyl-arene C–C bond forming reactions that allow regio and stereo control will most likely require the development of a reaction mechanism that does not involve formation of intermediate carbocations. Such a possible reaction is catalysis proceeds via the now well-known “CH activation” reaction to generate a phenyl-*M* species

* Corresponding author. Fax: +81-45-625-7272.

E-mail addresses: takaya.matsumoto@nmoc.co.jp (T. Matsumoto), rperiana@usc.edu (R.A. Periana).

¹ Fax: +1-213-821-2656.



Scheme 1.

that is well documented to be capable of reacting with olefins via non-carbocation reaction pathways to generate alkyl-arene products [3]. Given the ubiquity of the CH activation reaction [4–14], it could be assumed that such catalytic pathways would be well-known and already developed. However, in comparison to the large number of reported stoichiometric C–H bond activation reactions, relatively few catalytic systems have been reported. In the presence of an oxidant, Pd complexes catalyze oxidative vinylation of benzene with ethylene to produce styrene [15–17] or oxidative coupling of benzene to give biphenyl [18,19]. Ru complexes catalyze alkylation of aromatic ketones by olefins to afford products that are not easily obtainable by conventional synthetic methods. In this system, an acyl group (or other functional group) is required to activate the *ortho* C–H bonds of the aromatic ring for alkylation to occur [20–23]. Other related CH activation reactions of aromatics that require the presence of activating functional groups are the alkylation of pyridines and aromatic nitriles [24,25].

We have recently reported a homogeneous iridium complex that catalyzes the arylation of unactivated olefins with unactivated arenes to produce straight-chain alkylarenes with higher selectivity than the branched products, so-called anti-Markovnikov addition [1]. To our knowledge, this is the first efficient catalyst that shows this desirable high regioselectivity. Further details regarding the scope of the reaction with various arenes and olefins are described below.

2. Results and discussion

2.1. Reaction of arenes with olefins catalyzed by **1**

The binuclear Ir(III) complex $[\text{Ir}(\mu\text{-acac-O},\text{O}',\text{C}^3)(\text{acac-O},\text{O}')(\text{acac-C}^3)]_2$, **1**, (acac = acetylacetonato) has been shown to be an efficient catalyst for the anti-Markovnikov arylation of olefins with arenes

to produce alkylbenzenes. The results obtained for benzene and various olefins (Scheme 1) are given in Table 1. When benzene and complex **1** were heated in the presence of ethylene at 180 °C for 3 h, ethylbenzene was obtained (TOF = 0.0421 s⁻¹, TON = 455; entry 1 (TOF = turnover frequency, TON = turnover number)). Alkylation of benzene with propylene resulted in formation of *n*-propylbenzene and cumene in 61 and 39% selectivities, respectively (entry 3). Showing the generality of the reaction and the preference for anti-Markovnikov addition, reaction with 1-hexene and isobutene (entries 5 and 4) resulted in 1-phenylhexane (69% selectivity) and isobutylbenzene (82% selectivity), respectively. 3-Phenylpropionic acid methyl ester and 2-phenylpropionic acid methyl ester were also afforded by the reaction of benzene and methyl acrylate (68 and 32% selectivities, respectively; entry 6). Furthermore, in the reaction of benzene and styrene as an olefin, surprisingly 1,2-diphenylethane was afforded in 98% selectivity (entry 7).

It should be noted that these products are not readily obtainable by conventional Friedel–Crafts aromatic alkylation with olefins as in this case, reaction proceeds by Lewis and Brønsted acid activation of the olefin to produce branched alkylbenzenes in nearly 100% selectivity [26]. Indeed, even when shape selective, acidic zeolites are employed for Friedel–Crafts alkylations, it is almost impossible to obtain straight-chain alkylbenzene [27]. Typically, in order to synthesize straight chain alkyl aromatics, a combination of Friedel–Crafts acylation and Clemmensen reduction is employed. As a comparison, using AlCl₃ as a typical Friedel–Crafts catalyst, only Markovnikov addition products were observed at 50 °C (entries 12, 13 and 14). In order to compare Ir-catalyzed alkylation and Friedel–Crafts alkylation at the same temperature, reactant conversion and reaction rates, the heteropoly acid, H₃PW₁₂O₄₀ [28], (a mild Friedel–Crafts alkylation catalyst) was examined. As can be seen,

Table 1
Alkylation of benzene with various olefins^a

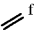
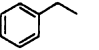
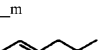

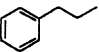
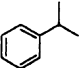
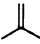
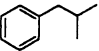
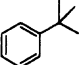

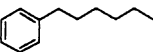
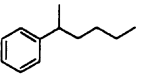
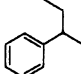
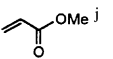
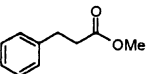
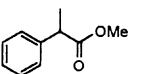
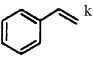
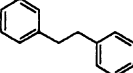
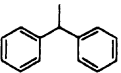
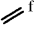
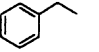

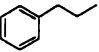
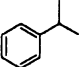
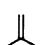
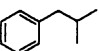
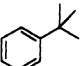

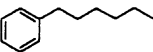
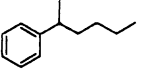
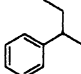
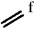
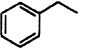

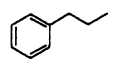
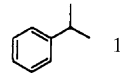
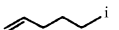
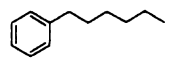
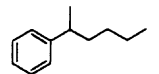
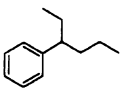
Entry	Catalyst	Olefin	Reaction time	TON ^b	TOF ^b ($\times 10^{-4} \text{ s}^{-1}$)	Product and selectivity (%) ^c		
1	1		3 h	455	421		1	
2	1		20 min	50	418		1	
3	1		20 min	13	110		61	 39
4	1		2 h	2	3		82	 18
5	1		20 min	8	69		69	 31  0
6	1		20 min	5	39		68	 32
7	1		20 min	22	180		98	 2
8	HPA ^d		20 min	11	87		1	
9	HPA ^d		20 min	579	4822		0	 100
10	HPA ^d		20 min	64	530		0	 100
11	HPA ^d		20 min	109	905		0	 66  34
12	AlCl ₃ ^e		20 min	26	218		1	

Table 1 (Continued)

Entry	Catalyst	Olefin	Reaction time	TON ^b	TOF ^b ($\times 10^{-4} \text{ s}^{-1}$)	Product and selectivity (%) ^c
13	AlCl ₃ ^e		20 min	95	795	 0  100
14	AlCl ₃ ^e		20 min	67	554	 0  66  34

^a Reaction temperatures are 180 °C for **1** and H₃PW₁₂O₄₀ and 50 °C for AlCl₃.

^b TON and TOF are based on Ir for **1** (TON = turnover number, TOF = turnover frequency).

^c Selectivity in mono-alkylated aromatic compounds.

^d H₃PW₁₂O₄₀.

^e AlCl₃ was conducted into an autoclave under N₂.

^f 1.96 MPa of ethylene.

^g 0.78 MPa of propylene, 1.96 MPa N₂.

^h 0.20 MPa of *i*-butene, 1.96 MPa N₂.

ⁱ Benzene/1-hexene solution containing 8.8 M of benzene. 1.96 MPa of N₂.

^j Benzene/methyl acrylate solution containing 10.1 M of benzene. 1.96 MPa of N₂.

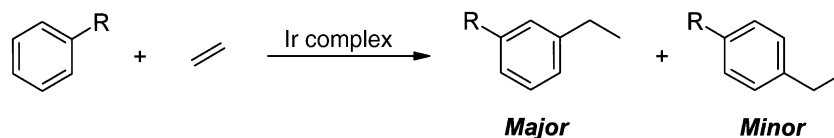
^k Benzene/styrene solution containing 9.9 M of benzene. 1.96 MPa of N₂.

^l [Ethylbenzene (EB)] = 279 mM, [diethylbenzene (DEB)] = 9 mM.

^m [EB] = 48 mM, [DEB] = 2 mM.

ⁿ [EB] = 13 mM, [DEB] = 1 mM.

^o [EB] = 426 mM, [DEB] = 20 mM.



Scheme 2.

consistent with the expected carbocation reaction mechanism, this catalyst also selectively gives the expected Markovnikov addition products (entry 8–11).

We also examined the reaction of various arenes with ethylene catalyzed by **1** (Scheme 2). As shown in Table 2, alkylation of toluene, instead of benzene, with ethylene gave only *m*- and *p*-ethylmethylbenzene in 63

and 37% selectivity: no *ortho* addition products were observed (entry 15). Similarly, ethylbenzene led to *m*- and *p*-diethylbenzene in a 7:3 ratio, respectively (entry 16). Conventional Friedel–Crafts alkylations with these substrates show a higher selectivity for the *o*- and *p*-addition products. Reaction with chlorobenzene and ethylene yielded, *o*-, *m*- and *p*-chloroethylbenzene

Table 2
Alkylation of various aromatic compounds with ethylene^a

Entry	Catalyst	Aromatic compound	Reaction time	TON ^b	TOF ($\times 10^{-4} \text{ s}^{-1}$) ^b	Product and selectivity (%) ^c		
15	1		20 min	22	186	37	63	0
16	1		20 min	26	214	30	70	0
17	1		20 min	13	104	31	63	6
18	1		20 min	0	0			
19	1		2 h	2	2	100	0	
20	HPA ^d		2 h	25	35	29	71	

^a 1.96 MPa of ethylene (reaction temperatures are 180 °C).

^b TON and TOF are based on Ir for **1**.

^c Selectivity in isomers.

^d H₃PW₁₂O₄₀.

^e Toluene saturated with water.

^f Ethylbenzene saturated with water.

^g Chlorobenzene saturated with water.

^h Pentafluorobenzene saturated with water.

ⁱ Naphthalene/*n*-heptane solution containing 0.5 M of naphthalene.

in 6, 63 and 31% selectivity, respectively (entry 17). The overall reactivity of chlorobenzene is lower than that of toluene and ethylbenzene, indicating that electronic withdrawing groups on the arene ring can retard reaction. Consistent with the possible deactivating influence of electronic drawing groups, pentafluorobenzene is an inert substrate (entry 18). A more thorough study of the effect of electron donating and withdrawing groups is currently underway. Interestingly, naphthalene was substituted at only β -position giving 2-ethylnaphthalene catalyzed by **1** (entry 19). As a comparison, using $\text{H}_3\text{PW}_{12}\text{O}_{40}$, α - and β -substitution were observed in 71 and 29% selectivity as expected from the relative stabilities of the expected intermediate carbocation resonance structures (entry 20).

The effect of varying the reaction time was explored for the alkylation of benzene with ethylene catalyzed by **1**. As shown in Fig. 1, the increase of TON for the production of ethylbenzene is linear with the reaction time under the condition of low concentration of product. This suggests that after 3 h at 180 °C, the catalyst shows no sign of instability under the reaction conditions even after >400 TON.

To determine the activation parameter, the TOF for the production of ethylbenzene were measured at various temperatures. The TOF for ethylbenzene increased from about 0.0017 s^{-1} at 140 °C up to 0.1304 s^{-1} at 200 °C. From the slope of the Arrhenius plot, Fig. 2, an activation energy of 28.7 kcal/mol was obtained.

We also measured the dependence of the rate of the alkylation on the ethylene/benzene ratio. This was done by varying the amount of ethylene. As can be seen in Fig. 3, the rate dependence on the ethylene/benzene molar ratio shows a “volcano” type relationship. The TOF initially rises with increasing ethylene/benzene ratio and drops after an ethylene/benzene ratio of ~ 0.20 . The initial rise is consistent with a non-zero order in ethylene while the drop in rate can be explained by reaction inhibition of a key mechanistic step by ethylene.

2.2. Comparison of catalysts

We screened a wide range of iridium complexes as catalysts for the alkylation of benzene with ethylene to produce ethylbenzene. As can be seen in Table 3, **1** is by far the most active catalyst for the reaction. Interestingly the rate for alkylation with $[\text{Ir}(\mu\text{-acac-O,O',C}^3)(\text{acac-O,O'})\text{Cl}]_2$, **2**, is significantly slower than that for **1** (entry 22). As expected, given the known stability of $\text{Ir}(\text{acac})_3$, it is inactive for the reaction at all (entry 23). We synthesized $[\text{Ir}(\text{bpym})\text{Cl}_4](\text{PPh}_4)$ (bpym = bipyrimidine), **3**, which should have an ability to capture and stabilize proton on the opposite side of bpym ligand to iridium, and examined it. However, of the complexes examined, only **1** and the related complex, **2**, show some activity for the alkylation reaction. As naked

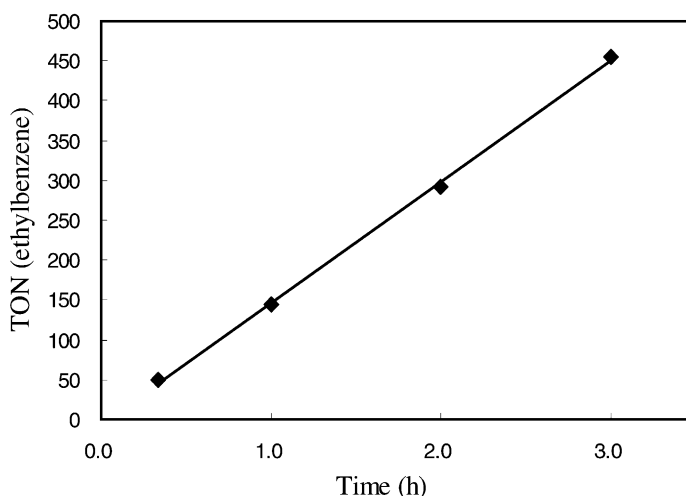


Fig. 1. The time dependence for alkylation of benzene with ethylene at 180 °C catalyzed by **1**.

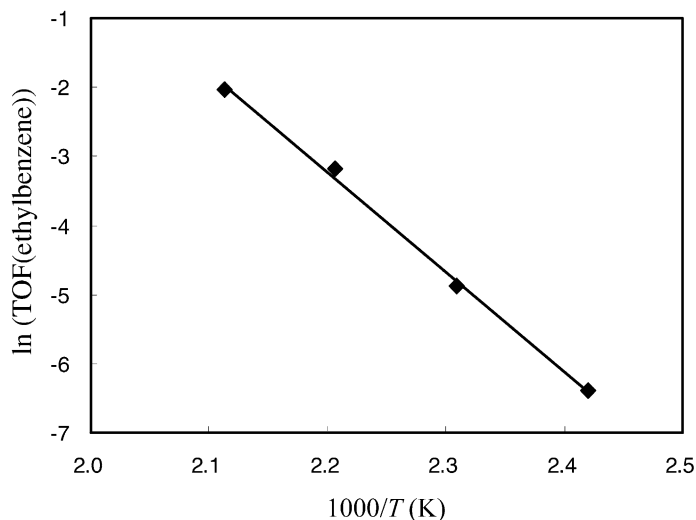


Fig. 2. The Arrhenius plot for alkylation of benzene with ethylene catalyzed by **1** (conditions: 200–140 °C, 20 min).

$\text{IrCl}_3 \cdot 3\text{H}_2\text{O}$ is also inactive, the existence of acac ligands and the specific geometry are required as a catalyst for the reaction.

2.3. Evidence against conventional Friedel–Crafts reaction

The observation that the olefin arylation occurs with greater selectivity for the straight chain product provides strong evidences that the reaction does not proceed via a Friedel–Crafts reaction mechanism. In

addition to different regioselectivity, other characteristics of the reaction of the olefin arylation catalyzed by **1** also provide evidence against a Friedel–Crafts reaction mechanism. Acid-catalyzed Friedel–Crafts alkylations of arenes with ethylene are typically slow compared to the reaction with substituted olefins because of the relative stabilities of the incipient carbocations. However, in the Ir-catalyzed alkylation reaction reported herein, ethylene reacts faster than substituted olefins. Additionally, transekylation between diethylbenzene and benzene to produce

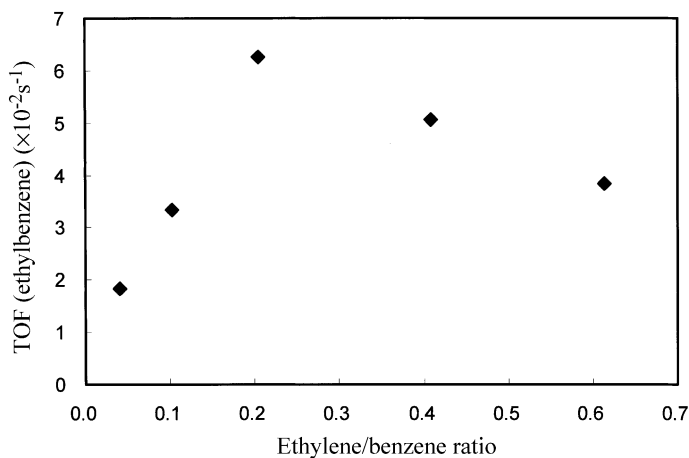


Fig. 3. The dependence of ethylene/benzene ratio for alkylation of benzene with ethylene at 180 °C catalyzed by **1**.

Table 3
Alkylation of benzene with ethylene^a

Entry	Catalyst	Ethylbenzene production	
		TON ^b	TOF ($\times 10^{-4} \text{ s}^{-1}$) ^b
21	1	157	1304
22	2	0.6	4.7
23	Ir(acac) ₃	0	0
24	IrCl ₃ ·3H ₂ O	0	0
25	[Ir(bpym)Cl ₄](PPh ₄), (3)	0	0
26	[Ir(bpy)Cl ₄](Hbpy)	0	0
27	[Ir(phen)Cl ₄](phen)	0	0
28	[Ir(ppy) ₂ Cl] ₂	0	0
29	[Ir(Cp*)Cl ₂] ₂	0	0
30	Ir(Cp*)(acac-O,O')Cl	0	0
31	Ir(Cp*)(acac-O,O')(acac-C ³)	0	0

32	Ir(acac)(CO) ₂	0	0
33	Ir(acac)(ethylene) ₂	0	0
34	[Ir(COD)Cl] ₂	0	0
35	[Ir(COD)(PPh ₂ Me) ₂](PF ₆)	0	0

^a Conditions: water saturated benzene, 1.10 mM of catalyst, 1.96 MPa of ethylene, 200 °C, 20 min.

^b TON and TOF are based on Ir.

ethylbenzene that is a classic test for Friedel–Crafts catalysts, is not catalyzed by **1**. Moreover the observation that the Ir-catalyzed reaction is accelerated by addition of water, (Table 4, entry 38) a known inhibitor of Lewis acid catalysts, is also not consistent with the reaction occurring via an olefin activation, carbocation type mechanism. We do not understand the basis for this rate acceleration by added water but note that the addition of a polar, non-nucleophilic solvent (perfluoropyridine, entry 37, Table 4) also leads to significant rate increase. It is possible that the

Table 4
Alkylation of benzene with ethylene catalyzed by **1**^a

Entry	Reaction media	Condition	TOF ($\times 10^{-4} \text{ s}^{-1}$) ^b
36	Distilled benzene	200 °C, 20 min	489
37	Distilled benzene/py-f ₅ (20 mM) ^c	200 °C, 20 min	1102
38	Benzene(H ₂ O sat.) ^d	200 °C, 20 min	1304
39	Benzene(H ₂ O sat.)/AcOH(58 mM) ^e	200 °C, 1 h	20
40	Benzene(H ₂ O sat.)/AcOH(175 mM) ^{e,f}	200 °C, 1 h	4

^a 1.96 MPa of ethylene.

^b TOF is based on Ir.

^c Distilled benzene/pentafluoropyridine solution.

^d Benzene saturated with H₂O.

^e Benzene saturated with H₂O/acetic acid glacial solution.

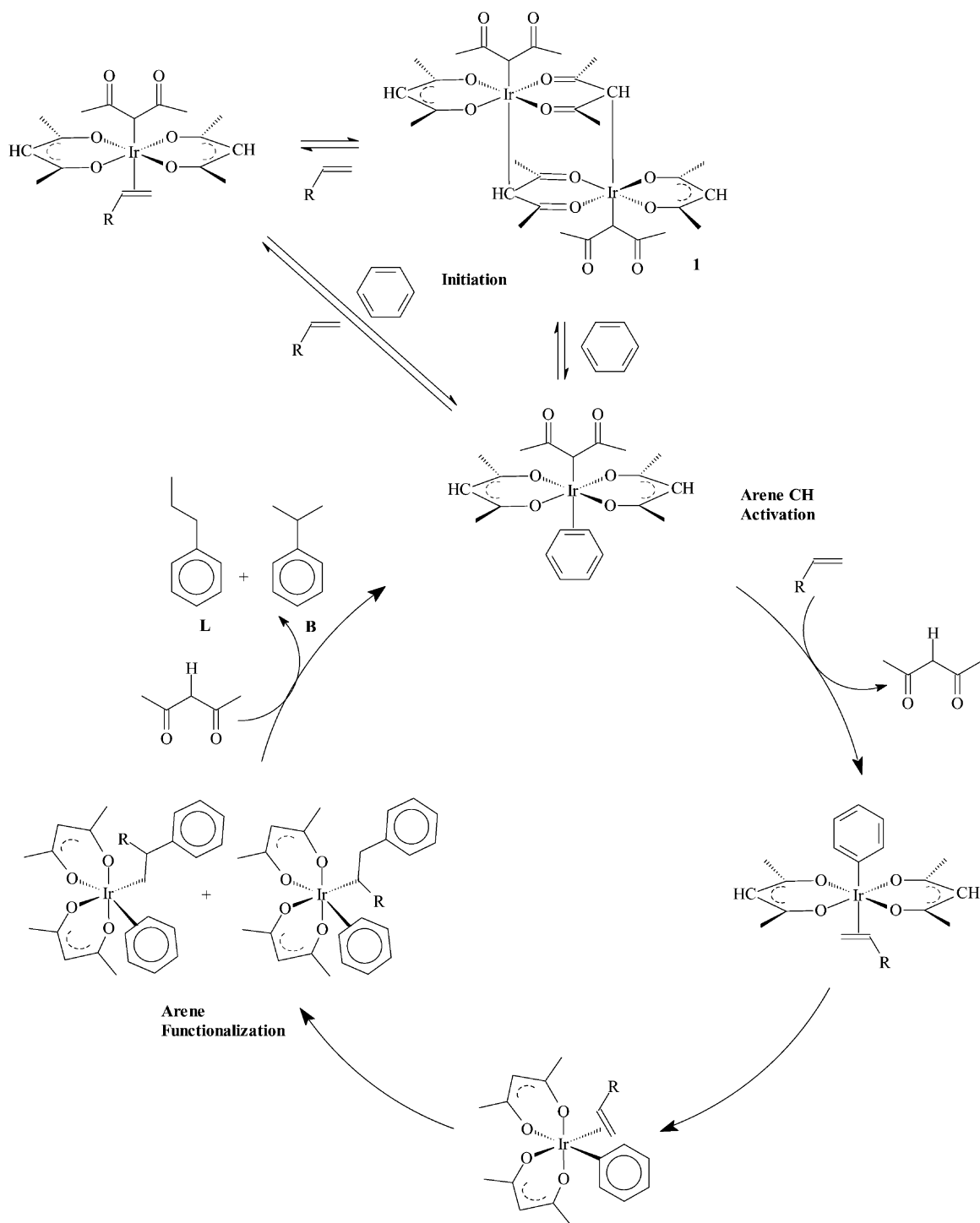
^f Entry 21: [EB] = 64 mM, [DEB] = 2 mM. Entry 22: [EB] = 99 mM, [DEB] = 3 mM. Entry 23: [EB] = 170 mM, [DEB] = 5 mM.

role of water is to similarly increase the solvent polarity. Interestingly, however, we note that the addition of acetic acid (entries 39 and 40) almost completely inhibits the alkylation reaction. A detailed kinetic study involving the effect of polarity and pH is underway to address these reaction details, as these could be possible paths for increasing reaction rates.

2.4. Proposed reaction mechanism

While we have no data on the detailed mechanism, it is likely that the reaction proceeds via CH activation. Further evidence that CH activation is a key step can be seen from the selective alkylation of toluene and other substituted arenes at the *meta*- and *para*-positions rather than the normal *ortho*, *para* attack. This selectivity, which is presumably driven by sterics, has also been observed in other CH activation systems. For example, toluene is activated in the *meta* and *para* positions by OsH(neopentyl)(PMe₃)₄ in statistical 2:1 ratio to produce Os–Ar species; no *ortho* products are observed [9].

Assuming that active catalyst is closely related to the complex added, **1**, and is an Ir(III) species, the important question of the composition and geometry of the catalytic species must be considered. Our current thinking is that the dimer (**1**) dissociates to generate two identical, coordinatively unsaturated Ir(III) complexes that is the species that activates benzene, coordinates olefin and subsequently generates the key species fac-(acac)₂Ir(RCHCH₂)(Ph), as shown in Scheme 3. This proposed dissociation of **1** is consistent with the X-ray structure of **1**, Fig. 4, which clearly



Scheme 3.

shows that the iridium–carbon bond to the bridging acac group are longer than the other bonds in the complex. The observation that complex **2** is less efficient than **1**, is consistent with the expectation that the dissociation of **2** would not be as facile as **1**. This is because in **1** the iridium–carbon bond to be broken is *trans* to a strong transabilizing group (a carbanion bound η^1 -acac) while in **2** the iridium–carbon bond is *trans* to a chloride. This important *trans* effect is clearly evident in Table 6 that shows that the iridium–carbon bond in the acac bridge is longer for complex **1** (2.32 Å) than complex **2** (2.22 Å).

However, it should be noted that while it would seem plausible that the active iridium catalyst is an Ir(III) species, the reaction conditions are reducing (ethylene and water are present) and an Ir(I) species can be generated in situ. However, based on the observation that electronic withdrawing groups tend (Cl or F, Table 2) to deactivate the arene ring to CH activation, it seems that an electrophilic substitution mechanism could be operating. We are currently attempting to isolate and synthesize the catalytic intermediates in an attempt to address these important issues.

2.5. Comparison to the Heck reaction

Additional evidence that a Friedel–Crafts mechanism can be ruled out in favor of a CH activation based mechanism can be obtained by comparisons of the branched to linear product ratios observed with **1** to that obtained from other transition metal catalyzed arene/olefin coupling reaction that are known to occur by non-Friedel–Crafts reaction mechanisms. The Heck reaction is the Pd(II) catalyzed reaction of aryl halides with olefins to generate unsaturated, vinylarenes. Under typical Heck reaction conditions, reaction of bromobenzene with propene yields 1-phenylpropene (linear product) and 2-phenylpropene (branched product) in approximately 70:30 ratio. This is almost identical to the linear to branched ratio we observed with catalyst **1** in spite of the differences in metal catalysts, reaction conditions and that our products are not olefinic.

An examination of the generally accepted mechanism for the Heck reaction provides a basis for this similarity. The Heck reaction is proposed to involve the rate determining activation of bromobenzene via a transition metal catalyst to generate a metal–phenyl

species as a key intermediate. In the case of **1**, we similarly propose the formation of a key metal–phenyl species but in this case via the activation of a C–H rather than a C–Br bond. While this can be expected to change the regioselectivity with respect to the arene ring, this difference would not be expected to lead to differences in the branched to linear product ratios if this selectivity is determined after the arene activation step. In the Heck reaction, the arene activation step is followed by olefin insertion that is proposed to determine the linear to branched product ratios. Subsequent β -hydride elimination and olefin formation in the Heck reaction is assumed to be fast and not expected to influence the linear to branched product ratio. Similarly, we propose that olefin insertion into the metal–phenyl species followed by alkyl arene formation determines the linear to branched ratio.

In Scheme 3, we propose that a $\text{PhCH}_2\text{CHR-Ir}$ bonded intermediate in a key species in the catalytic pathway. It is well-known, especially from studies carried out on homogeneous catalysts for olefin polymerization, that metal–alkyl intermediates with CH bonds β to the metal tend to undergo β -hydride eliminations to generate olefin metal hydrides that can lead to formation of olefin products, Scheme 4. While the reaction of olefin with arene to generate styrenes are uphill (2.94 kcal/mol at 100 °C), Scheme 5, the reaction with two equivalents of olefin, Scheme 6, is quite favorable (–19.06 kcal/mol at 100 °C).²

Consequently, if the β -hydride reaction did occur, it would be reasonable to see some aryl olefin materials under our reaction conditions. We see no evidence for olefin formation and at least in the cases examined, we see no evidence for catalyst (due to possible irreversible formation of olefin metal hydrides) decomposition even after >400 turn-overs. A plausible consideration is that since the catalyst is a relatively electron poor Ir(III) complex (with hard oxygenic ligands) the β -hydride elimination is not thermodynamically favorable, as olefin complexes are not stable on such electron poor centers. We are currently examining the synthesize and characterization of olefin complexes on the proposed $\text{Ir}(\text{acac})_2$ core.

² Calculated by HSC Chemistry for Windows Version 4.0 program, Chemical Reaction and Equilibrium Software with Extensive Thermochemical Database, Outokumpu Research Oy Information Service, Finland.

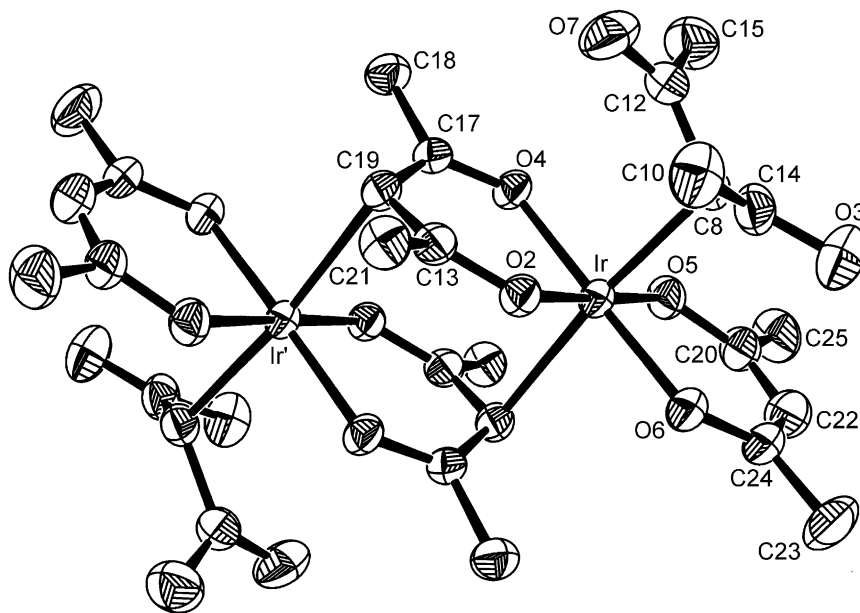
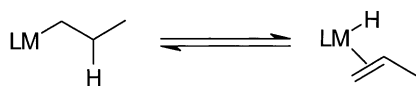
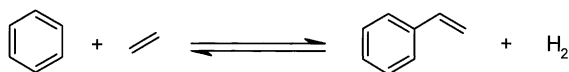


Fig. 4. Structure of $[\text{Ir}(\mu\text{-acac-O,O',C}^3)(\text{acac-O,O}')(\text{acac-C}^3)]_2$ (**1**).



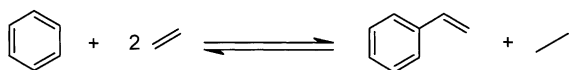
Scheme 4.



Scheme 5.

2.6. X-ray structure of **1**

Bennett and Mitchell isolated **1** as a by-product in the course of an attempt to improve the synthesis of $\text{Ir}(\text{acac})_3$. They determined the structure of **1** from NMR, IR and elemental analysis, although no catalysis with **1** was reported [29]. We determined the crystal structure of **1** using a single crystal X-ray diffraction analysis, in which *p*-xylene was contained as a lattice



Scheme 6.

solvent. The crystal data is shown in Table 5. The crystal structure of complex **1** is displayed in Fig. 4, whereas bond lengths and bond angles are collected in Table 6. As Bennett proposed, **1** is a dinuclear Ir(III) complex with three different types of coordinated acac ligands; a conventional bidentate, O-bonded acac, a γ -C-bonded acac and a bridging acac ligand that connects the two Ir centers via an Ir–O, O' to one metal center and an Ir–C bond from the central carbon of the acac ligand to the second Ir center. In contrast to the distances of Ir–O(2), Ir–O(4), Ir–O(5) and Ir–O(6) (2.011–2.039 Å), those of Ir–O(7) and Ir–O(3) (3.577(6) and 3.755(6) Å) are quite long and obviously not within bonding distance. Therefore, the terminal acac coordinates to Ir by only γ -carbon. In a related complex, $\text{KPt}(\text{acac-O,O}')(\text{acac-C}^3)\text{Cl}$ [30], which has γ -C-bonded acac, is known. However, although Ir(III) complex having γ -C-bonded acac, $\text{IrCp}^*(\text{acac-O,O}')(\text{acac-C}^3)$ [31], is also known, no X-ray structural study for the geometry has been reported. This is the first example to reveal the structure of γ -C-bonded acac ligated to Ir(III).

The Ir–C(19') distance of 2.329(6) Å is much longer than normal Ir–C σ -bond [32,33], which usually falls in the range around 2.00–2.02 Å. The length is close to

Table 5
Crystal data and details of the structure determination for **1**, **2** and **3**

	1	2	3
Formula	C ₃₀ H ₄₂ O ₁₂ Ir ₂	C ₂₀ H ₂₈ O ₈ C ₁₂ Ir ₂	C ₃₂ H ₂₆ N ₄ IrCl ₄ P
Formula weight	979.09	851.78	831.59
Crystal system	Triclinic	Monoclinic	Triclinic
Space group	<i>P</i> $\bar{1}$ (no. 2)	<i>P</i> 2 ₁ / <i>n</i> (no. 14)	<i>P</i> $\bar{1}$ (no. 2)
Crystal color	Yellow	Yellow	Red
<i>a</i> (Å)	8.394(1)	7.992(2)	17.965(3)
<i>b</i> (Å)	14.177(2)	12.613(2)	21.715(8)
<i>c</i> (Å)	8.089(2)	11.855(2)	16.652(3)
α (°)	93.20(2)	90	90.01(2)
β (°)	96.77(2)	91.24(1)	90.01(2)
γ (°)	98.74(1)	90	89.66(2)
<i>V</i> (Å ³)	942.1(3)	1194.8(3)	6495(2)
<i>Z</i>	1	2	8
<i>D</i> (calcd.) (g cm ⁻³)	1.726	2.367	1.701
<i>F</i> (000)	472.00	800.00	3248.00
μ (Mo K α) (cm ⁻¹)	71.27	114.24	45.29
Crystal size (mm)	0.10 × 0.02 × 0.10	0.20 × 0.20 × 0.20	0.15 × 0.10 × 0.04
2 θ range (°)	5 < 2 θ < 55	5 < 2 θ < 55	6 < 2 θ < 55
Temperature (°C)	23.0	23.0	23.0
Radiation (Å)	0.71069 (Mo K α)	0.71069 (Mo K α)	0.71069 (Mo K α)
No. of total data measured	4612	3070	14542
No. of observed unique data	4086(2 σ)	2042 (2 σ)	8949(2 σ)
Residual electron density (e/Å ³)	0.67	3.29	8.26
No. of parameters	235	154	673
<i>R</i> ^a	0.035	0.056	0.097
<i>Rw</i> ^b	0.037	0.061	0.129
<i>w</i>	1/ σ^2 (<i>F</i>)	1/ σ^2 (<i>F</i>)	1/ σ^2 (<i>F</i>)
GOF	0.74	1.49	1.89

$$^a R = \sum ||F_o| - |F_c|| / \sum |F_o|.$$

$$^b Rw = [\sum w(|F_o| - |F_c|)^2 / \sum w|F_o|^2]^{1/2}.$$

Ir-C(sp²) π -bond (2.27–2.31 Å) [34] rather than Ir-C σ -bond, as seen in Ir(III)-cyclooctadiene complex. Compared to this, the Ir–C(8) distance is 2.165(6) Å, which suggests bond breaking of Ir–C(19') is easier, as discussed above, leading to the dissociation of the dimer structure and generations of a 5-coordinate, Ir(III) species that allows the CH activation reaction.

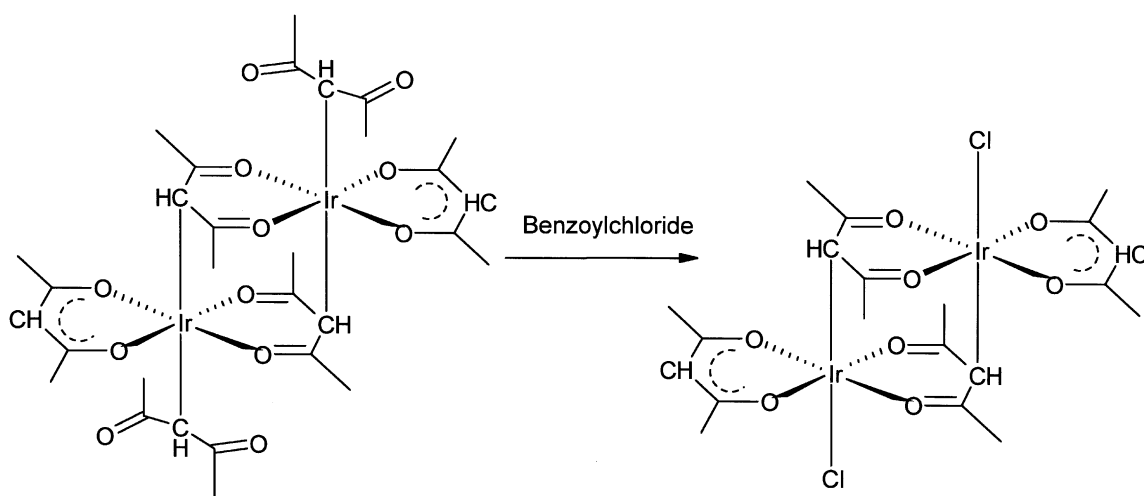
As shown in Table 8, complex **1** shows three different types of ν (CO) bands, a set of 1669 and 1653 cm⁻¹, 1594 cm⁻¹ and a pair of 1555 and 1525 cm⁻¹, respectively assigned for γ -C-bonded acac, bridging acac and bidentate O-bonded acac, which are consistent with bond lengths.

2.7. Synthesis and X-ray structure of **2**

Addition of a large excess of benzoyl chloride to **1** at ambient temperature gave complex **2** in 74% yield in which the γ -C-bonded acac group to the Ir center is replaced by chloride (Scheme 7). Complex **2** was characterized by ¹H NMR, ¹³C NMR, IR, FD–MS, elemental analysis and X-ray analysis. The ¹H NMR spectrum of **2** shows two methyl singlets and two methine singlets, each in 1:1 ratio. The ¹³C NMR spectrum exhibits two sets of methyl, methine and carbonyl signals. These NMR data suggest that **2** has two types of symmetrical acac groups. As shown in Table 8, the

Table 6
Major bond distances and angles for **1**

Distances (Å)			
Ir(1)–O(2)	2.032(4)	Ir(1)–O(4)	2.039(4)
Ir(1)–O(5)	2.018(4)	Ir(1)–O(6)	2.011(4)
Ir(1)–C(19)	2.329(6)	Ir(1)–C(8)	2.165(6)
O(2)–C(13)	1.270(7)	O(4)–C(17)	1.267(7)
O(5)–C(20)	1.280(8)	O(6)–C(24)	1.281(8)
O(3)–C(14)	1.226(8)	O(7)–C(12)	1.225(9)
C(13)–C(19)	1.439(9)	C(17)–C(19)	1.443(9)
C(22)–C(24)	1.39(1)	C(20)–C(22)	1.39(1)
C(8)–C(12)	1.505(10)	C(8)–C(14)	1.485(10)
Angles (°)			
O(2)–Ir(1)–O(4)	93.2(2)	O(2)–Ir(1)–O(5)	178.4(2)
O(2)–Ir(1)–O(6)	86.4(2)	O(2)–Ir(1)–C(8)	92.3(2)
O(2)–Ir(1)–C(19)	92.4(2)	O(4)–Ir(1)–O(5)	85.6(2)
O(4)–Ir(1)–O(6)	178.8(2)	O(4)–Ir(1)–C(8)	91.9(2)
O(4)–Ir(1)–C(19)	92.2(2)	O(5)–Ir(1)–O(6)	94.7(2)
O(5)–Ir(1)–C(8)	86.6(2)	O(5)–Ir(1)–C(19)	88.8(2)
O(6)–Ir(1)–C(8)	87.0(2)	O(6)–Ir(1)–C(19)	89.0(2)
C(8)–Ir(1)–C(19)	173.5(2)		
Torsion angles (°)			
O(4)–C(17)–C(19)–C(13)	24(1)		
O(2)–C(13)–C(19)–C(17)	–25(1)		
O(3)–C(14)–C(8)–C(12)	43.3(2)		
O(7)–C(12)–C(8)–C(14)	–43(1)		
O(5)–C(20)–C(22)–C(24)	3(1)		
O(6)–C(24)–C(22)–C(20)	–1(1)		



Scheme 7.

Table 7

Major bond distances and angles for **2**

Distances (Å)			
Ir(1)–O(3)	2.03(1)	Ir(1)–O(4)	2.05(1)
Ir(1)–O(1)	2.01(1)	Ir(1)–O(6)	2.01(1)
Ir(1)–C(1)	2.22(2)	Ir(1)–Cl(1)	2.377(4)
O(4)–C(10)	1.27(2)	O(3)–C(14)	1.25(2)
O(6)–C(9)	1.28(2)	O(1)–C(17)	1.26(2)
C(10)–C(1)	1.46(2)	C(14)–C(1)	1.47(2)
C(9)–C(12)	1.40(2)	C(17)–C(12)	1.39(2)
Angles (°)			
O(4)–Ir(1)–O(3)	92.1(4)	O(4)–Ir(1)–O(6)	175.1(5)
O(4)–Ir(1)–O(1)	87.6(4)	O(4)–Ir(1)–Cl(1)	88.5(4)
O(4)–Ir(1)–C(1)	93.0(6)	O(3)–Ir(1)–O(6)	85.7(4)
O(3)–Ir(1)–O(1)	178.0(5)	O(3)–Ir(1)–Cl(1)	89.3(4)
O(3)–Ir(1)–C(1)	94.2(6)	O(6)–Ir(1)–O(1)	94.6(4)
O(6)–Ir(1)–Cl(1)	87.0(4)	O(6)–Ir(1)–C(1)	91.6(6)
O(1)–Ir(1)–Cl(1)	88.7(5)	O(1)–Ir(1)–C(1)	87.8(6)
Cl(1)–Ir(1)–C(1)	176.1(4)		
Torsion angles (°)			
O(3)–C(14)–C(1)–C(10)		–27(3)	
O(4)–C(10)–C(1)–C(14)		29(3)	
O(6)–C(9)–C(12)–C(17)		5(3)	
O(1)–C(17)–C(12)–C(9)		1(4)	

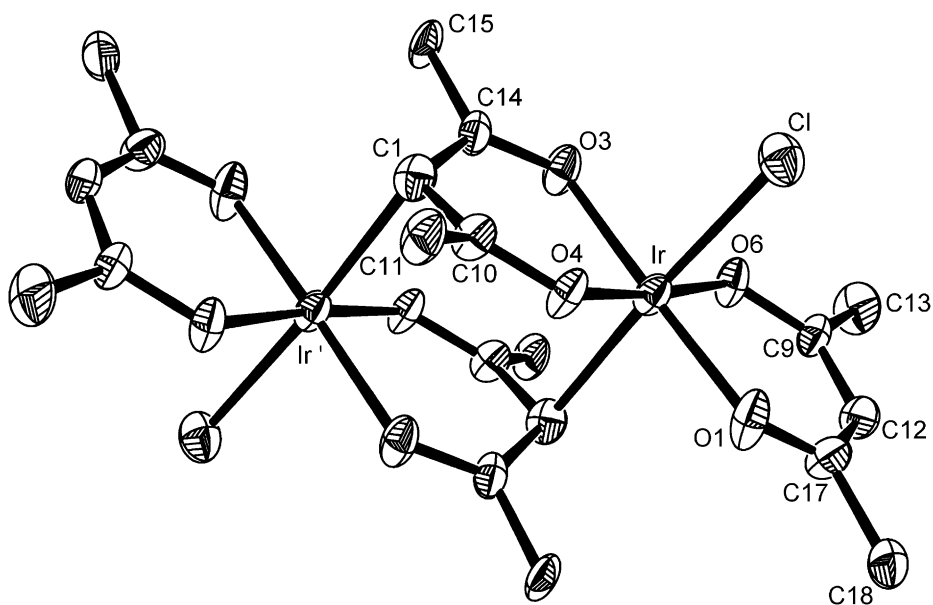
Fig. 5. Structure of $[\text{Ir}(\mu\text{-acac-O,O',C}^3)(\text{acac-O,O'})\text{Cl}]_2$ (**2**).

Table 8
CO stretching vibration and CO bond distance

Complex	$\nu(\text{CO})$ (cm^{-1}) IR/(Raman)			CO bond length (\AA)		
	C-acac ^a	B-acac ^b	O-acac ^c	C-acac ^a	B-acac ^b	O-acac ^c
1	1669, 1653 (1669, 1657)	1594 (1574)	1555, 1525 (1555, 1527)	1.226, 1.225	1.270, 1.267	1.281, 1.280
2		1611 (1592)	1557, 1538 (1556)		1.25, 1.27	1.26, 1.28
.....						
IrH(acac)(C ₂ H ₃)(PiPr ₃) ₂			1590, 1515 ^d			1.28, 1.28 ^d
[RhCp*(acac-O,O',C ³) ₂ (BF ₄) ₂					1.260, 1.252 ^e	
KPt(acac-O,O')(acac-C ³)Cl	1678, 1634 ^f		1560, 1518 ^f	1.16, 1.21 ^f		1.33, 1.27 ^f
Pd(acac-O,O')(acac-C ³)(py)	1680, 1640 ^g		1568, 1521 ^g			

^a C-bonded acac.

^b Bridging acac.

^c Bidentate O-bonded acac.

^d Data from [33].

^e Data from [31].

^f Data from [30].

^g Data from [35].

IR spectrum of **2** shows a pair of $\nu(\text{C}=\text{O})$ bands at 1538 and 1557 cm^{-1} and a $\nu(\text{C}=\text{O})$ band at 1611 cm^{-1} that are characteristic of a bidentate O-bonded acac group and a bridging acac group. No $\nu(\text{C}=\text{O})$ band in the region higher than 1640 cm^{-1} that would correspond to γ -C-bonded acac group is observed [31,35]. The FD-MS shows a parent peak at 851. These data support the binuclear structure of **2**. We also determined the structure by a single crystal X-ray diffraction method, in which water was included as a lattice solvent. The crystal data is shown in Table 5, and bond lengths and bond angles are collected in Table 7. As can be seen in Fig. 5, **2** is a binuclear Ir(III) complex analogous to complex **1**. The Ir-C(1) bond from the Ir center to the central carbon of the second acac ligand is 2.22(2) \AA , which is shorter than 2.329(6) \AA of complex **1**. As a relevant reaction, Pd(acac-O,O')(acac-C³)py, which has a γ -C-bonded acac group, reacts with benzoyl chloride to give Pd(acac-O,O')(py)Cl [35].

3. Experimental section

3.1. General

GC analyses were performed with a Shimadzu GC-17A gas chromatograph equipped with an FID detector and a crosslinked methyl silicone gum capillary column, PONA. GC-MS analyses were

performed with a Hewlett-Packard HP5971A GC-MS system equipped with crosslinked methyl silicone gum capillary column, PONA. ¹H NMR spectra were recorded on a JEOL EX-270 (270 MHz), a JEOL EX-400 (400 MHz) and a Bruker ARX-300 (300 MHz) instruments. ¹³C NMR spectra were recorded on a JEOL EX-270 (68 MHz), a JEOL EX-400 (101 MHz) instruments with complete proton decoupling. Infrared spectra were measured on a Perkin Elmer Spectrum 2000 instrument. Raman spectra were recorded on a Perkin Elmer Spectrum 2000 instrument. The excitation source was 1064 nm line of an Nd:YAG laser. FD-MS spectra were measured on a JEOL HX-110 and a JEOL AX-505 instruments. FAB-MS spectra were obtained on a JEOL HX-110 instrument. The samples were measured as nitrobenzyl alcohol solutions. Elemental analyses were performed at the Analytical Group, Central Technical Research Laboratory, Nippon Mitsubishi Oil Corporation. Single-crystal X-ray diffraction analysis was conducted at Mitsui Chemicals Analytical Center Inc.

[Ir(bpy)Cl₄](Hbpy), [Ir(phen)Cl₄](Hphen), [Ir(ppy)₂Cl]₂, Ir(Cp*)(acac-O,O')Cl and Ir(Cp*)(acac-O,O')(acac-C³) were prepared by literature methods [31, 36–38]. [Ir(Cp*)Cl₂]₂, Ir(acac)(CO)₂, and [Ir(COD)(PPh₂Me)₂](PF₆) were purchased from Aldrich Chemical Co. Ir(acac)₃ and [Ir(COD)Cl]₂ were purchased from Strem Chemicals, Inc. Ir(acac)(ethylene)₂ was purchased from Colonial Metals, Inc.

3.2. Reaction procedures

The product yields were determined by GC (FID) analyses using chlorobenzene as an internal standard that was introduced into the reaction solution after reaction. The retention times of products were confirmed by standards. Products were also qualitatively determined by GC–MS analyses. The compounds as GC standards for retention time are commercially available except 2-phenylpropionic acid methyl ester, 3-phenylpropionic acid methyl ester, 2-phenylhexane and 3-phenylhexane. The 2-phenylpropionic acid methyl ester used for a GC standard was synthesized from esterification of 2-phenylpropionic acid and excess of methanol catalyzed by HCl. The 3-phenylpropionic acid methyl ester used for a GC standard was synthesized from esterification of 3-phenylpropionic acid and excess of methanol catalyzed by HCl. The 2-phenylhexane was obtained as a mixture of 1-phenylhexane and 2-phenylhexane from scaled up alkylation of benzene with 1-hexene catalyzed by **1**. Furthermore, all four compounds as above were in the library of Hewlett-Packard HP5971A GC–MS system.

3.3. Olefin arylation

A 10 ml stainless autoclave, equipped with a glass insert and a magnetic stir bar was charged with 3 ml of benzene saturated with water and 1.0 mg of **1**. The reactor was degassed with nitrogen, pressurized with 1.96 MPa of ethylene and heated to 180 °C with stirring for 3 h. The liquid phase was sampled and analyzed by GC (FID) and GC–MS at the end of the reaction. All other arylation reactions were performed by similar procedures.

By administering the ethylene from known-volume, known-pressure reservoirs into the reactor, the molar ratio of ethylene and benzene could be controlled. In a typical procedure for the reaction with known amount of ethylene, the reactor is degassed by nitrogen, pressurized with various amounts of ethylene, and sequentially pressurized with nitrogen up to a total pressure of 2.94 MPa. We employed 0.20, 0.49, 0.98, 1.96 and 2.94 MPa of ethylene, which correspond to 0.04, 0.10, 0.20, 0.41 and 0.61 of ethylene/benzene ratios. For the detailed condition, see supporting information.

3.4. Synthesis of complex **1**

Complex **1** was prepared by literature procedure [29]. Yellow crystals of **1** were obtained by recrystallization from dichloromethane/cyclooctane and *p*-xylylene. Abbreviations: O-acac: O-bonded acac; C-acac: γ -C-bonded acac; B-acac: bridging acac. ¹H NMR (270 MHz, δ , CDCl₃): 5.51 (s, 1H, CH), 5.08 (s, 1H, CH), 5.07 (s, 1H, CH), 1.99 (s, 3H, CH₃), 1.96 (s, 3H, CH₃), 1.91 (s, 3H, CH₃). ¹³C NMR (68 MHz, δ , CDCl₃): 212.7 (C-acac C=O), 203.0 (B-acac C=O), 184.6 (O-acac C=O), 103.2 (O-acac CH), 62.1 (B-acac CH), 39.8 (C-acac CH), 32.2 (C-acac CH₃), 29.9 (B-acac CH₃), 27.2 (O-acac CH₃). IR (KBr): 1669 (w), 1653 (m), 1594 (m), 1555 (s), 1525 (s). Raman: 1669 (s), 1657 (s), 1574 (s), 1555 (sh, w), 1527 (br, w). FD–MS: 979 (*M*⁺), 489 (1/2*M*⁺). Anal. Calcd. for C₃₀H₄₂O₁₂Ir₂: C, 36.80; H, 4.32. Found: C, 36.69; H, 4.41.

3.5. Synthesis of complex **2**

Benzoyl chloride (4 ml) was added to a solid sample of complex **1** (0.146 g, 0.150 mmol). The yellow suspension was stirred under nitrogen at ambient temperature for 24 h. Over the course of reaction, the color of the suspension turned to orange. Diethyl ether (40 ml) was introduced into the suspension, and an orange solid was isolated by filtration. Recrystallization from CH₂Cl₂/diethyl ether gave **2** as an orange microcrystalline. The yield was 74%. ¹H NMR (270 MHz, δ , CDCl₃): 5.74 (s, 1H, CH), 5.66 (s, 1H, CH), 2.17 (s, 3H, CH₃), 2.13 (s, 3H, CH₃). ¹³C NMR (68 MHz, δ , CDCl₃): 212.7 (B-acac C=O), 186.4 (O-acac C=O), 103.1 (O-acac CH), 44.7 (B-acac CH), 30.6 (B-acac CH₃), 26.5 (O-acac CH₃). IR (KBr): 1611 (s), 1557 (s), 1538 (s). Raman: 1592 (s), 1556 (br, w). FD–MS: 851 (*M*⁺). Anal. Calcd. for C₂₀H₂₈Cl₂O₈Ir₂: C, 28.20; H, 3.31. Found: C, 28.53; H, 3.42.

3.6. Synthesis of [Ir(*bpym*)Cl₄](PPh₄) (*bpym* = bipyrimidine), **3**

A solution of 2,2'-bipyrimidine (0.548 g, 3.46 mmol) in hot water (40 ml) containing concentrated hydrochloric acid (0.04 ml) was added to a solution of iridium trichloride hydrate (0.400 g, 1.13 mmol) in water (20 ml) including hydrochloric acid (5 ml).

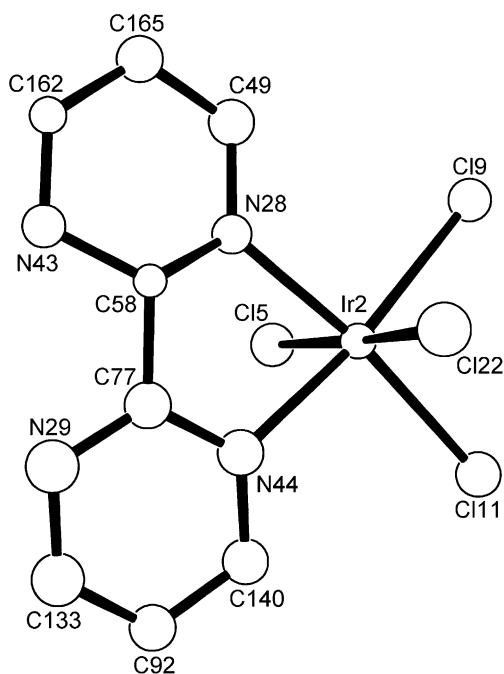


Fig. 6. Structure of $[\text{Ir}(\text{bpym})\text{Cl}_4]^-$ ($[\mathbf{3}]^-$).

The mixture was refluxed for 2 h. After cooling, a solution of tetraphenylphosphonium chloride (1.276 g, 3.40 mmol) in water (20 ml) was slowly added to the reaction solution. Then the obtained solution was left sitting at ambient temperature for 24 h during which time red needle-like crystals and some black precipitate were generated. Filtered and washed with water to remove the black precipitate which is soluble in water, the red crystals of **3** were isolated. The yield was 54%. Anal. Calcd. for $\text{C}_{32}\text{H}_{26}\text{N}_4\text{Cl}_4\text{Ir}_1$: C, 46.22; H, 3.15; N, 6.74; Cl, 17.15. Found: C, 45.93; H, 3.25; N, 6.67; Cl, 17.11. Raman ($\nu(\text{Ir}-\text{Cl})$): 324 (m), 309 (m), 282 (m). The structure of **3** was confirmed by single crystal X-ray diffraction method. The crystal data is shown in Table 5. As can be seen in Fig. 6, complex **3** has a non-bridging bpym ligand and is a monomeric structure.

3.7. Collection and reduction of X-ray data

Crystals of **1**, **2** and **3** were subjected to single-crystal X-ray diffraction analysis. Unit cell parameters for **1** and **3** were obtained from a least-squares refinement

of 25 reflections in the range $29.57^\circ < 2\theta < 29.95^\circ$. Unit cell parameters for **2** were obtained from a least-squares refinement of 19 reflections in the range $29.17^\circ < 2\theta < 29.86^\circ$. All measurements were made on a Rigaku AFC7R diffractometer with graphite monochromated Mo $K\alpha$ radiation and a rotating anode generator. Over the course of data collection for complex **1**, the standards decreased by 5.0%. The standards decreased by 5.2% through data collection for complex **2**. An increase of 0.3% was observed for the standards of **3**. A linear correction factor was applied to the data to account for this phenomenon regarding these measurements. The Lorentz polarization correction was made to the collected data.

3.8. Solution and refinement of the structure

The structures of **1** and **3** were solved by heavy-atom Patterson methods (PATTY [39]) and expanded using Fourier techniques (DIRDIF94 [40]). The structures of **2** was solved by direct methods (SIR92 [41]) and expanded using Fourier techniques (DIRDIF94). In the analyses of **1** and **2**, the non-hydrogen atoms were refined anisotropically. Hydrogen atoms were included, but their positions were not refined; isotropic B values were refined. Because of low crystallinity and difficulty with recrystallization due to quite low solubility, the atoms of **3** were refined isotropically. The final cycle of full-matrix least-squares refinement was based on observed reflections with unweighted and weighted agreement factors ($R = \sum ||F_o| - |F_c|| / \sum |F_o|$ and $R_w = [\sum w(|F_o| - |F_c|)^2 / \sum w|F_o|^2]^{1/2}$). All calculations were performed using the TeXsan [42] crystallographic software package. The ORTEP images were drawn by the Ortep-3 for Windows [43] software.

4. Conclusion

We report the details of the anti-Markovnikov olefin arylation reaction, catalyzed by the Ir complex, **1**. A wide range of olefins and arenes can be employed for the synthesis of alkyl arenes. Coupled with the unique higher selectivity for the formation of linear alkylarenes several observations suggest that the reaction does not proceed by a Friedel–Crafts type reaction pathway involving carbocations: (i) acceleration of the reaction by water, (ii) no disproportionation

between diethylbenzene and benzene and (iii) the observation that the reaction with ethylene is faster than that with substituted olefins. The mechanism of the reaction has not yet been fully elucidated, but appears to involve phenyl CH activation by Ir to form an Ir–phenyl species. This conclusion is based primarily on that the linear to branched alkylarene product ratio is very similar to that observed in the Heck reaction, where a Pd–phenyl species is proposed to be a key intermediate.

Acknowledgements

We thank Prof. Henry Taube, Prof. R.H. Crabtree and Prof. A. Streitwieser for discussion.

References

- [1] T. Matsumoto, D.J. Taube, R.A. Periana, H. Taube, H. Yoshida, *J. Am. Chem. Soc.* 122 (2000) 7414.
- [2] K.B. Jensen, J. Thorhauge, R.G. Hazell, K.A. Jørgensen, *Angew. Chem. Int. Ed.* 40 (2001) 160.
- [3] R.F. Heck, *J. Am. Chem. Soc.* 90 (1968) 5518.
- [4] R. Zhou, C. Wang, Y. Hu, T.C. Flood, *Organometallics* 16 (1997) 434.
- [5] A.D. Selmezy, W.D. Jones, R. Osman, R.N. Perutz, *Organometallics* 14 (1995) 5677.
- [6] T.Y. Meyer, K.A. Woerpel, B.M. Novak, R.G. Bergman, *J. Am. Chem. Soc.* 116 (1994) 10290.
- [7] W.D. Jones, E.T. Hessell, *J. Am. Chem. Soc.* 114 (1992) 6087.
- [8] W.T. Boese, A.S. Goldman, *Organometallics* 10 (1991) 782.
- [9] T.C. Flood, in: G.A. Olah, K. Wade, R.E. William (Eds.), *Electron Deficient Boron Carbon Clusters*, Wiley, New York, 1991, p. 324 (Chapter 13).
- [10] I.V. Kozhevnikov, V.I. Kim, E.P. Talzi, V.N. Sidelnikov, *J. Chem. Soc. Chem. Commun.* (1985) 1392.
- [11] R.V. Helden, G. Verberg, *Rec. Trav. Chim.* 84 (1965) 1263.
- [12] E. Gretz, T.F. Oliver, A. Sen, *J. Am. Chem. Soc.* 109 (1987) 8109.
- [13] P. Hong, H. Yamazaki, *J. Mol. Catal.* 26 (1984) 297.
- [14] R.H. Crabtree, *Chem. Rev.* 85 (1985) 245.
- [15] Y. Fujiwara, I. Moritani, S. Danno, R. Asano, S. Teranishi, *J. Am. Chem. Soc.* 91 (1969) 7166.
- [16] V.E. Taraban'ko, I.V. Kozhevnikov, K.I. Matveev, *Kinet. I. Katal.* 19 (1978) 1160.
- [17] R.F. Heck, in: R.J. Adams (Ed.), *Organic Reactions*, Wiley, New York, 1982, p. 345 (Chapter 2).
- [18] H. Iataaki, H. Yoshimoto, *J. Org. Chem.* 38 (1973) 76.
- [19] A.I. Rudenkov, G.U. Mennenga, L.N. Rachkovskaya, K.I. Matveev, I.V. Kozhevnikov, *Kinet. I. Katal.* 18 (1977) 915.
- [20] S. Murai, N. Chatani, F. Kakiuchi, *Pure Appl. Chem.* 69 (1997) 589.
- [21] S. Murai, F. Kakiuchi, S. Sekine, Y. Tanaka, A. Kamatani, M. Sonoda, N. Chatani, *Nature* 366 (1993) 529.
- [22] F. Kakiuchi, S. Sekine, Y. Tanaka, A. Kamatani, M. Sonoda, N. Chatani, S. Murai, *Bull. Chem. Soc. Jpn.* 68 (1995) 62.
- [23] B.M. Trost, K. Imi, I.W. Davies, *J. Am. Chem. Soc.* 117 (1995) 5371.
- [24] Y.G. Lim, J.S. Han, B.T. Koo, J.B. Kang, *Bull. Korean Chem. Soc.* 20 (1999) 1097.
- [25] F. Kakiuchi, M. Sonoda, T. Tsujimoto, N. Chatani, S. Murai, *Chem. Lett.* (1999) 1083.
- [26] E.E. Burgoyne, *A Short Course in Organic Chemistry*, McGraw-Hill, Singapore, 1985, p. 137.
- [27] Y. Cao, R. Kessas, C. Naccache, Y.B. Taarit, *Appl. Catal. A* 184 (1999) 231.
- [28] T. Okuhara, T. Nishimura, H. Watanabe, M. Misono, *J. Mol. Catal.* 74 (1992) 247.
- [29] M.A. Bennett, T.R.B. Mitchell, *Inorg. Chem.* 15 (1976) 2936.
- [30] B.N. Figgis, J. Lewis, R.F. Long, R. Mason, R.S. Nyholm, P.J. Pauling, G.B. Robertson, *Nature* 195 (1962) 1278.
- [31] W. Rigby, H.-B. Lee, P.M. Bailey, J.A. McCleverty, P.M. Maitlis, *J. Chem. Soc. Dalton* (1979) 387.
- [32] Z. Lu, C.-H. Jun, S.R. de Gala, M. Sigalas, O. Eisenstein, R.H. Crabtree, *Ir(PPh₃)₂(biph)Cl*, *Organometallics* 14 (1995) 1168.
- [33] B. Papenfuhs, N. Mahr, H. Werner, *IrH(CH=CH₂)(acac)(PiPr₃)₂*, *Organometallics* 12 (1993) 4244.
- [34] T. Yoshida, K. Tani, T. Yamagata, Y. Tatsuno, T. Saito, *[IrH(COD){Fe[η⁵-C₅H₃(2-C₅H₄N)](η⁵-C₅H₄PPh₂)]PF₆*, *J. Chem. Soc. Chem. Commun.* (1990) 292.
- [35] S. Baba, T. Ogura, S. Kawaguchi, *Bull. Chem. Soc. Jpn.* 47 (1974) 665.
- [36] R.A. Cipriano, L.R. Hanton, W. Levason, D. Pletcher, N.A. Powell, M. Webster, *J. Chem. Soc. Dalton* (1988) 2483.
- [37] M. Nonoyama, K. Yamasaki, *Inorg. Nucl. Chem. Lett.* 7 (1971) 943.
- [38] F.O. Garces, K.A. King, R.J. Watts, *Inorg. Chem.* 27 (1988) 3464.
- [39] PATTY by P.T. Beurskens, G. Admiraal, G. Beurskens, W.P. Bosman, S. Garcia-Granada, R.O. Gould, J.M.M. Smits, C. Smykalla, *The DIRDIF program system*, Technical Report of the Crystallography Laboratory, University of Nijmegen, The Netherlands, 1992.
- [40] DIRDIF94 by P.T. Beurskens, G. Admiraal, G. Beurskens, W.P. Bosman, R. de Gelder, R. Israel, J.M.M. Smits, *The DIRDIF94 program system*, Technical Report of the Crystallography Laboratory, University of Nijmegen, The Netherlands, 1994.
- [41] A. Altomare, M. Cascarano, C. Giacovazzo, A. Guagliardi, *J. Appl. Cryst.* 26 (1994) 343.
- [42] *Crystal Structure Analysis Package*, Molecular Structure Corporation, 1985–1999.
- [43] L.J. Farrugia, *J. Appl. Cryst.* 30 (1997) 565.